Title
THE INVESTIGATION OF PARTON FRAGMENTATION WITH THE TPC DETECTOR AT PEP: RECENT RESULTS

Author
Hofmann, W.

Publication Date
1985-08-01

Lawrence Berkeley Laboratory

UNIVERSITY OF CALIFORNIA

Physics Division

Presented at the International Symposium on
Multiparticle Dynamics, Kiryat Anavim, Israel,
June 1985

THE INVESTIGATION OF PARTON FRAGMENTATION WITH THE TPC DETECTOR AT PEP: RECENT RESULTS

W. Hofmann

August 1985

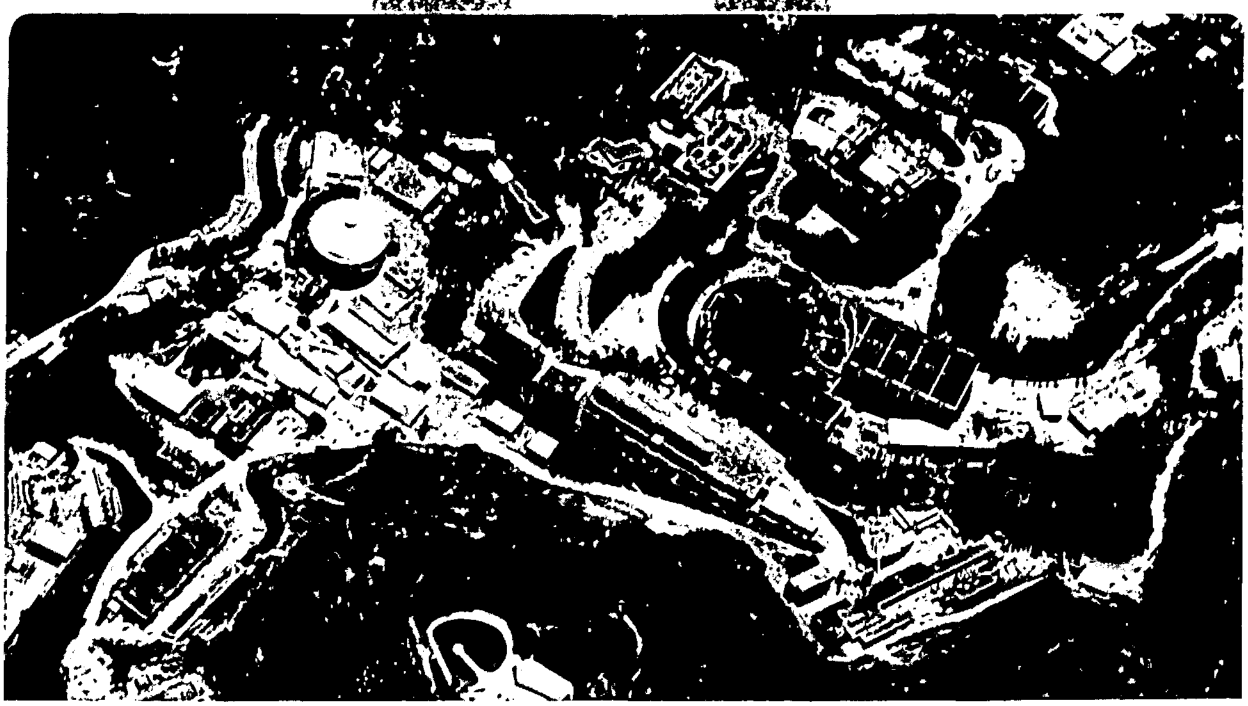

Prepared for the U.S. Department of Energy under Contract DE-AC03-76SF00098

The Investigation of Parton Fragmentation with the TPC Detector at PEP - Recent Results

Werner Hofmann
Lawrence Berkeley Laboratory
University of California
Berkeley, CA 94720

Representing the PEP4/PEP9 TPC Collaboration

August 1985

Presented at the Int. Symposium on Multiparticle Dynamics,
Kiryat Anavim, Israel, 1985

ABSTRACT

Long-range correlations are discussed as a new tool to test the parton model and jet universality and are used to determine general properties of quark fragmentation functions. Proton-antiproton correlations and proton rapidity distributions yield information about details of the confinement process, excluding e.g. the decay of heavy mesonic clusters as the dominant source of baryons.

This talk will cover some of our recent studies of the mechanisms of quark fragmentation in e^+e^- annihilation; most results are based on the investigation of two- or multiparticle correlations.

I will first discuss the study of long-range (or "forward-backward") correlations as a new tool in the investigation of parton fragmentation. Since the details of measurement[1)] and formalism[1,2)] are published, I give here only a brief overview. Using the sphericity axis, each event is divided into two jets. For a given (absolute) rapidity y (or any other kinematic variable), the $\pi^{\pm}$ cross section is measured simultaneously in opposite jets (Fig. 1(a)). We distinguish two types of cross sections: singlets S (which are invariant under charge conjugation), such as $D_q^{\pi^+} + D_q^{\pi^-}$ (expressed in terms of quark fragmentation functions D), and non-singlets N (which change sign) such as $D_q^{\pi^+} - D_q^{\pi^-}$. Rewriting those expressions as $D_q^{\pi^+} + D_{\overline{q}}^{\pi^+}$ and $D_q^{\pi^+} - D_{\overline{q}}^{\pi^+}$, we see that singlets measure the sum of quark and antiquark fragmentation functions, whereas non-singlets measure their difference. In e^+e^- annihilation, only singlets can be measured directly. The non-singlets, however, are most interesting quantities - they tell us which particles carry the quantum numbers of the quark initiating a jet.

In QCD, we expect factorisation of quark and antiquark fragmentation functions. For a two-particle cross section measured at the same y in opposite jets, this implies $D(y,y) = D_q(y)D_{\overline{q}}(y)$. From Fig. 1(b), it is obvious that the two-particle non-singlet cross-section $N(y,y)$ measures the negative square of the non-singlet fragmentation function: $N(y,y) = -N^2(y)$. We will present results in terms of the ratio $\sqrt{-N(y,y)}/S(y)$ of non-singlet and singlet fragmentation functions. The singlet two-particle cross-section yields another interesting piece of information. Using the the two-particle and single-particle cross sections we derive a correlation function $C = S(y,y) - S^2(y)$. Let us for the moment concentrate on the simplest singlet quantity: the multiplicity of charged particles in a jet. If particle multiplicities in the q and the $\overline{q}$ jet are uncorrelated, we expect C=0. If, however, light-quark and heavy-quark jets have different mean particle multiplicities, we will observe a positive correlation (Fig. 1(c)). A more detailed discussion shows indeed that the $\sqrt{C}/S$ measures the relative rms variation of a given (singlet) fragmentation property among quark flavors. Another interesting aspect is that under the assumption of factorization, the signs of the two-particle corss sections are uniquely predicted: negative for non-singlets and positive for singlet correlation functions. Any violation of these conditions would indicate dynamical long-range correlations in the fragmentation process and would cast a shadow of doubt on our use of the quark parton model and QCD.

The extraction of the two-particle pion densities avoiding artificial correlations due to detector acceptance or event selection criteria is non-trivial and is described in 1). All two particle densities were found to have the correct sign; we assume therefore that factorization holds. The main results - the ratios of non-singlet to singlet fragmentation functions and the relative rms variation of singlet fragmentation functions over quark flavors as a function of scaled energy x and rapidity y - are presented in Fig. 2(a)-(d). We observe that the importance of non-singlet contributions (Fig. 2(a),(b)) increases with x and y, indicating that the quantum numbers (in this case, charge or isospin) of the primary quark are carried preferentially by high-momentum particles. The slight rise at low y is caused by tails of short-range correlations. Significant differences between quarks are observed for the singlet fragmentation functions (Fig. 2(c),(d)), in agreement with results obtained using quark tagging methods. The data is well described by the LUND fragmentation model[3)].

The same technique can be used to study other fragmentation properties. We find e.g. that the mean transverse momenta of hadrons in quark jets varies by less than 10% (at 90% C.L.) with the flavor of the primary quark.

The study of baryon production in e^+e^- annihilation provides a valuable tool for the investigation of finer details of the confinement mechanism. We exploit angular correlations between protons and antiprotons to distinguish between different phenomenological descriptions of baryon production[4)].

Hadron production in e^+e^- annihilation is usually pictured as indicated in Fig. 3(a): new quarks are created in the color field of the primary $q-\overline{q}$ pair (points labeled 1) and combine to form mesons M. Baryons are often incorporated by means of diquark-antidiquark production (point 2 in Fig.3(b)). In one class of models, diquarks are introduced as more or less fundamental entities[5)]. Other models[6)] provide a dynamical description of how effective diquarks can be formed (Fig. 3(c)). It is argued that occasionally $q-\overline{q}$ pairs of the wrong, non-screening color are produced in the confining color field (point 3). In order to screen the remaining field, another $q-\overline{q}$ pair (point 4) has to be produced. A more detailed discussion of the forces involved shows that the quarks created in points 3 and 4 form loosely bound diquarks, resulting in the production of a baryon and an antibaryon. In such a scheme, baryon and antibaryon are not necessarily neighbors in rank; quite often more than one $q-\overline{q}$ pair is created in the remaining field, and one or more mesons are produced in between baryon and antibaryon (Fig. 3(d)). Technically, the latter mechanism is equivalent to models with diquarks which break up through the process[7)] diquark $\rightarrow$ diquark + meson.

An entirely different approach is provided by QCD models, where a parton shower creates low-mass color singlet clusters, some of which may be heavy enough to decay into a baryon and an antibaryon. In the following, we compare these mechanisms for baryon production. We use the LUND model[3)] as a typical color-string diquark scheme, and the Webber model[8)] as an example for the QCD cluster approach.

Despite their fundamental differences, both string and cluster models reproduce the measured inclusive proton spectra quite well[4)]. However, the model predictions for the angular dependence of proton-antiproton correlations differ qualitatively. Consider the distribution of θ^*, the angle between the baryon momentum vector and the sphericity axis of the event, measured in the rest frame of the $p\overline{p}$ pair. If baryons are produced in the decay of unpolarised mesonic clusters, the distribution in

$\cos\theta^*$ will be flat. There may be a small non-isotropic contribution due to pairs where p and $\bar{p}$ come from different clusters; the rate of this background equals the rate of pp and $\bar{p}\bar{p}$ combinations and can easily be subtracted. In string models with diquarks, diquark (qq) and anti-diquark $(\overline{qq})$ are pulled apart by the tension of the color string. Therefore the $p\bar{p}$ momentum difference has a tendency to align with the jet axis, and the distribution in $\cos\theta^*$ will peak near $|\cos\theta^*| \cong 1$ (Fig. 4(a)). In our analysis, only protons between 0.5 GeV/c and 1.5 GeV/c momentum could be used. Fig. 4(b) shows the data and the model predictions with the same cuts as applied to the data. Whereas data are consistent with the behaviour expected for diquark models (full curve), the cluster model (dashed) is excluded at 95% C.L.. A possibly cure (somewhat against the "perturbative spirit" of the model) is to introduce baryonic clusters by allowing diquark-antidiquark pairs to be created in the parton shower.

Angular correlations in the plane perpendicular to the jet axis discriminate between the variants of the diquark picture. If diquarks are quasi-stable entities, baryon and antibaryon will recoil against each other, reflecting the fact that in a one-dimensional color force field (qq) and $(\overline{qq})$ will be produced with opposite transverse momenta[3)]. If mesons are created in the color field between the (qq) and the $(\overline{qq})$, this angular correlation is largely destroyed[6,9)].

We define a correlation coefficient $\alpha = \langle \vec{p}_{T,p}\vec{p}_{T,\bar{p}} \rangle / \langle \vec{p}_T^{\,2} \rangle$. Apart from the basic production mechanism, the value of α is influenced by resonance decays, errors in the determination of the event axis etc.. The most drastic change is due to events with radiative gluons: here p and $\bar{p}$ are emitted from a moving string segment and experience a common boost, which induces a positive $\vec{p}_T$ correlation. The experimental sensitivity improves considerably if α is calculated using the momentum components p_{out} out of the event plane instead of $\vec{p}_T$.

In Fig. 5, the correlation coefficients α_{out} and α_{in} are contrasted with predictions diquark models, where mesons (M) may form in between a baryon (B) and the antibaryon $(\overline{B})$. The predictions are shown as a function of the probability f for such a $BM\overline{B}$ configuration. For small f, the $p,\bar{p}$ momentum components out of the event plane tend to have opposite signs. This value of α is extremely insensitive to details of the modeling, such as the implementation of the perturbative part (2^{nd} order QCD or parton showers), or the detailed values of model parameters. With increasing f, boost effects dominate, resulting in a positive value of α. For string models, we derive the lower limit $f > 45\%$ at 90% C.L..

Another source of valuable information on baryon production in the confinement process are decays of the upsilon meson. Measurements[10)] show a large increase in the baryon rates on the Υ as compared to the nearby continuum. String phenomenology[3)] provides a natural explanation for this phenomenon: for Υ decays into three gluons, the configuration of the color field resembles a closed loop, and baryons can be produced anywhere along that loop. In $q\bar{q}$ events, on the other hand, the color string is spanned by the primary $q\bar{q}$ pair. For a variety of (partly kinematical) reasons, baryon production is expected to be suppressed near the ends of the string[3,6], resulting in a lower total baryon rate. This model can be tested using TPC data on π, k and p rapidity distributions at 29 GeV. The study of inclusive cross sections as a function of rapidity has the advantage that particle production in the confining gluon field (central rapidity region) and in the vincinity of the primary quarks (fragmentation region) can be investigated separately, provided the energy is large enough to allow a separation of these regions. Fig. 6 shows the measured distributions, together with model predictions for the total π, k, and p distributions, the distribution if charm and bottom decay products are excluded, and the distribution if particles stemming from a primary quark (rank-1 particles) are excluded. At $y \cong 0$, the contribution of such particles is small, as expected. It is also obvious that rank-1 particles contribute much more to total pion and kaon rates than to proton rates. We concentrate on particle fractions, in order to avoid problems with the relative normalization. We find the following ratios: $(p+\bar{p})/\pi^{\pm} = 0.074 \pm 0.008$ in e^+e^- annihilation at $y = 0$ compared to 0.068±0.010 on the Υ, $(\Lambda+\Lambda)/\pi^{\pm} = 0.018 \pm 0.003$ compared to 0.022 ± 0.003 and $k^{\pm}/\pi^{\pm} = 0.105 \pm 0.012$ compared to 0.161±0.024. From this point of view, there is certainly no evidence for an unnatural enhancement of baryon production on the Υ. Kaon production appears to be enhanced; however the Υ data is somewhat problematic, in that the kaon rates are measured only in a small momentum range and are extrapolated to obtain total kaon multiplicities. Using the better-measured k^0 instead of $k^{\pm}$, the ratio drops to 0.120 ± 0.016, consistent with our value.

In summary, long range correlations are presented as a new tool to extract properties of quark fragmentation functions, and to study the variation of fragmentation properties among quark flavors. Inclusive proton distributions and proton-antiproton correlations are used to test details of models for baryon production, resulting in a very good agreement of string models with data.

This work was supported by the U.S. Department of Energy under contract number DE-AC03-76SF00098.

REFERENCES

1. H. Aihara et al., Z. f. Phys. C27, 495 (1985).
2. P. Hoyer, Proc. XIV Int. Symp. on Multiparticle Dynamics, Granlibakken, 1983, p. 100.
3. B. Andersson et al., Phys. Rep. 97, 31 (1983); T. Sjostrand, Com. Phys. Comm.27, 243 (1982), 28, 229 (1983).
4. For more details see: H. Aihara et al., LBL-19566 (1985).
5. B. Andersson, G. Gustafson, T. Sjostrand, Nucl. Phys. B197, 45 (1982); T. Meyer, Z. f. Phys. C12, 77 (1982).
6. A. Casher, H. Neuberger, S. Nussinov, Phys. Rev. D20, 179 (1979); B. Andersson, G. Gustafson, T. Sjostrand, LU TP 84-9 (1984) (unpublished).
7. E.M. Ilgenfritz, J. Kripfganz, A. Schiller, Acta Phys. Pol. B9, 881 (1978); A. Bartl, H. Fraas, W. Majoretto, Phys. Rev. D26, 1061(1982).
8. B.R. Webber, Nucl. Phys. B238, 492 (1984).
9. A. Bartl et al., Phys. Lett. 122B, 427 (1983).
10. S. Behrends et al., Phys. Rev. D31, 2161 (1985).
11. P. Allen et al., Nucl. Phys. B214, 369 (1983).

FIGURE CAPTIONS

1. a) Schematic: measurement of long-range correlations;
b) Typical singlet and nonsinglet densities for a 2-jet event, vs rapidity;
c) Typical correlation of forward and backward hadron multiplicities in light-quark and heavy quark events.

2. a,b) open squares: ratio of non-singlet over singlet fragmentation functions for pions as a function of scaled energy x and rapiditiy y, respectively. Crosses in a): non-singlet/singlet ratio from νN and $\overline{\nu} N$ interactions[11]. Dotted lines: contributions due to tails of short range correlations, estimated using the LUND Monte-Carlo. c,d) Relative rms variation of singlet fragmentation functions for pions vs x and y.

3. Schematic representation production mechanisms:
(a) Meson production via $q - \overline{q}$ creation and recombination.
(b) Baryon production via diquark-antidiquark creation.
(c) Creation of diquark-like systems as a two-step process.
(d) As (c), but with meson production in between baryon and antibaryon.

4. Normalized distribution of $p\overline{p}$ pairs in the angle θ^* between the proton direction and the sphericity axis, measured in the $p\overline{p}$ rest frame, after subtraction of like-sign combinations. (a) predictions of the LUND diquark model with stable diquarks (full lines) and of the Webber cluster model (dashed lines). For the mechanism of Figs. 3(c),(d), the LUND predictions will increase slightly for $\cos\theta^* \cong 1$. (b) Experimental distribution in θ^* of $p\overline{p}$ pairs where the p and $\overline{p}$ momenta are in the 0.5 - 1.5 GeV/c range. Full and dashed lines: model predictions (as in (a)).

5. Correlation coefficient α of $p, \overline{p}$ momentum components out of the event plane (a) and in the event plane (b). Shaded bands: data ± 1 S.D.. Full lines: model predictions as a function of the probability f to find a $BM\overline{B}$ configuration instead of $B\overline{B}$.

6. Inclusive rapidity distributions for $\pi^{\pm}$ (a), $k^{\pm}(b)$ and $p, \overline{p}(c)$. Full lines: predictions of the LUND Monte Carlo. Dashed: predictions excluding charm and bottom decay products. Dot-dashed: predictions excluding rank-1 hadrons.

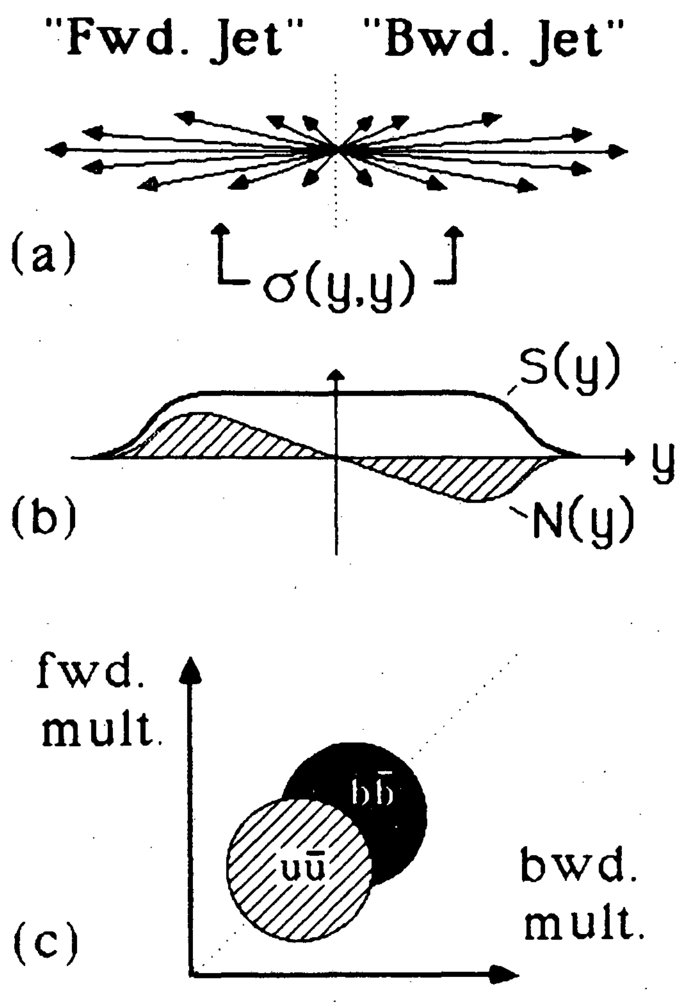

Fig. 1

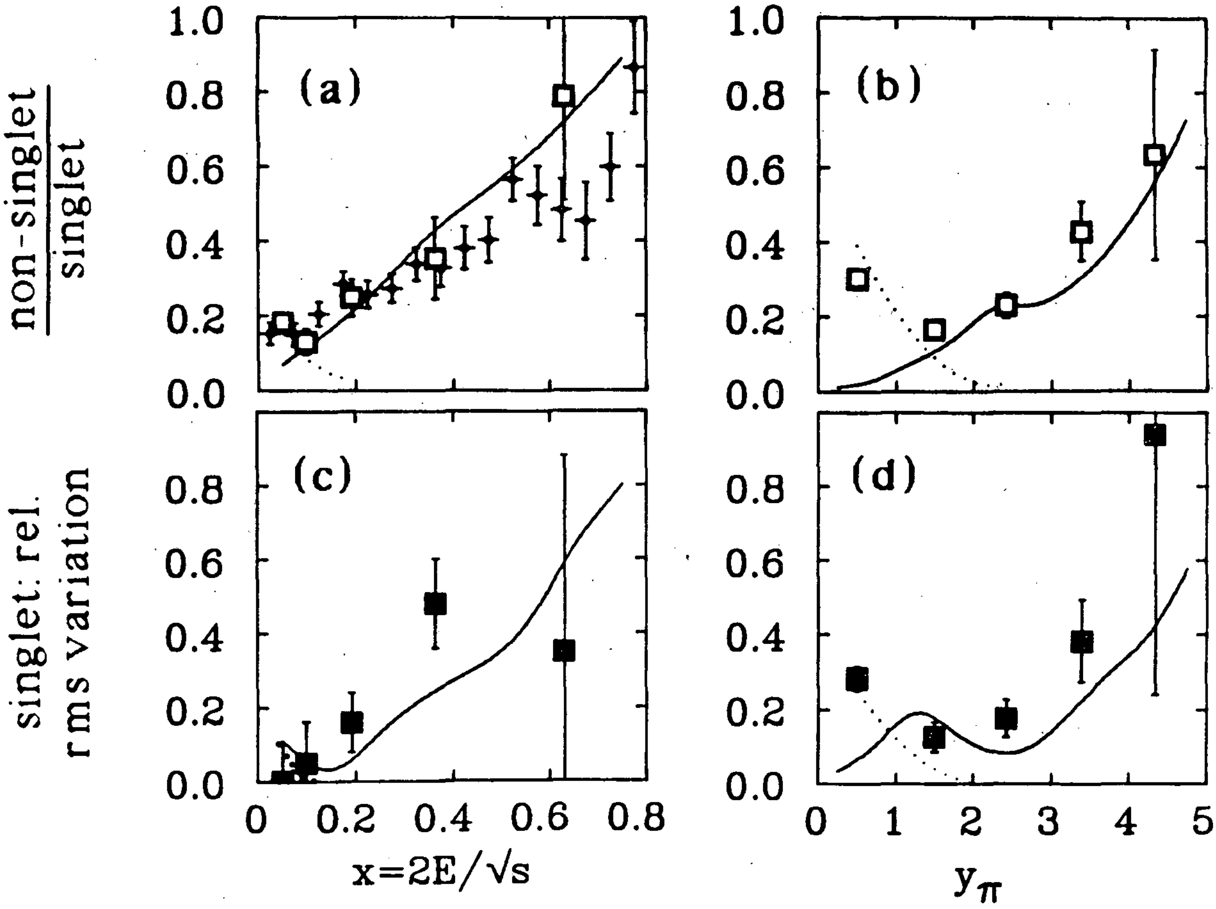

(a)
(b)
(c)
(d)
non-singlet / singlet
singlet: rel. rms variation
x=2E/√s
y_π
1.0
0.8
0.6
0.4
0.2
0.0
0
0.2
0.4
0.6
0.8
1
2
3
4
5

Fig. 2

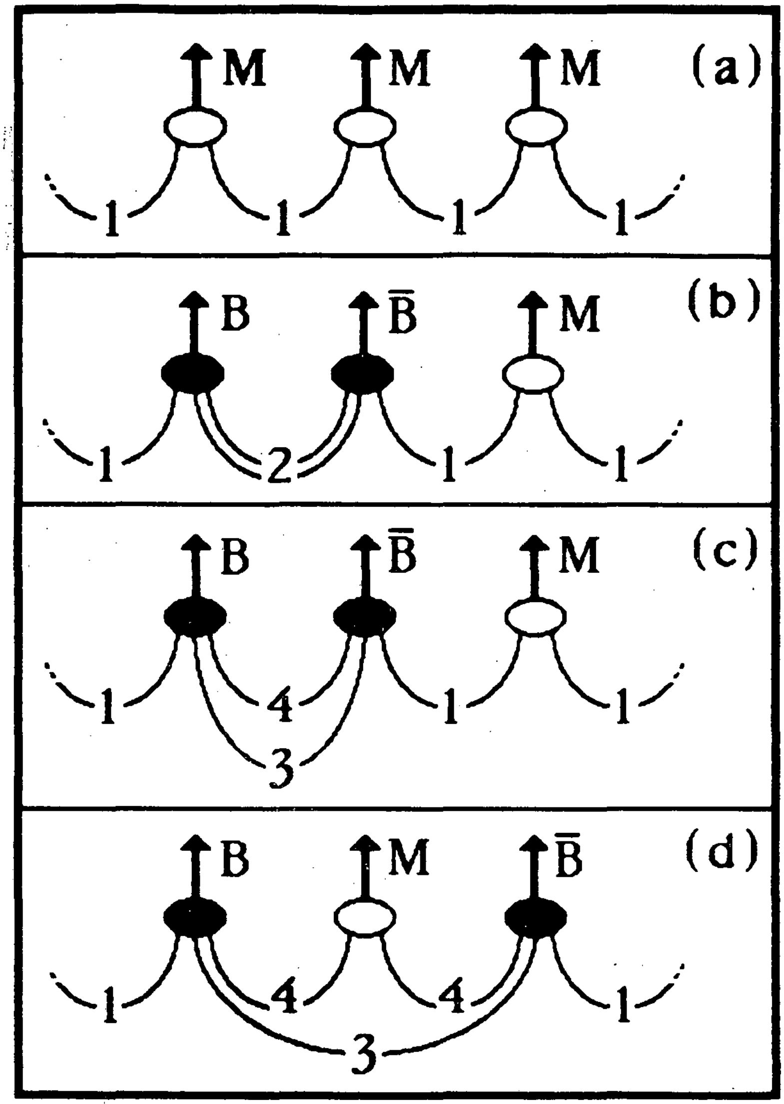

Fig. 3

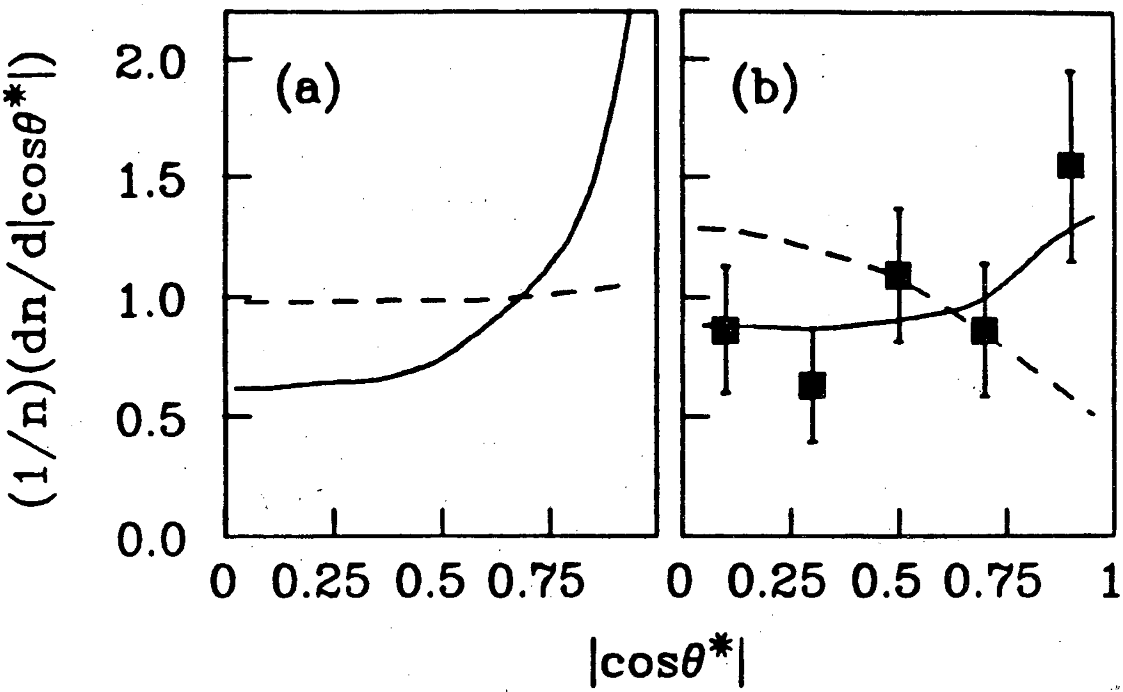

Fig. 4

XBL 854-2314

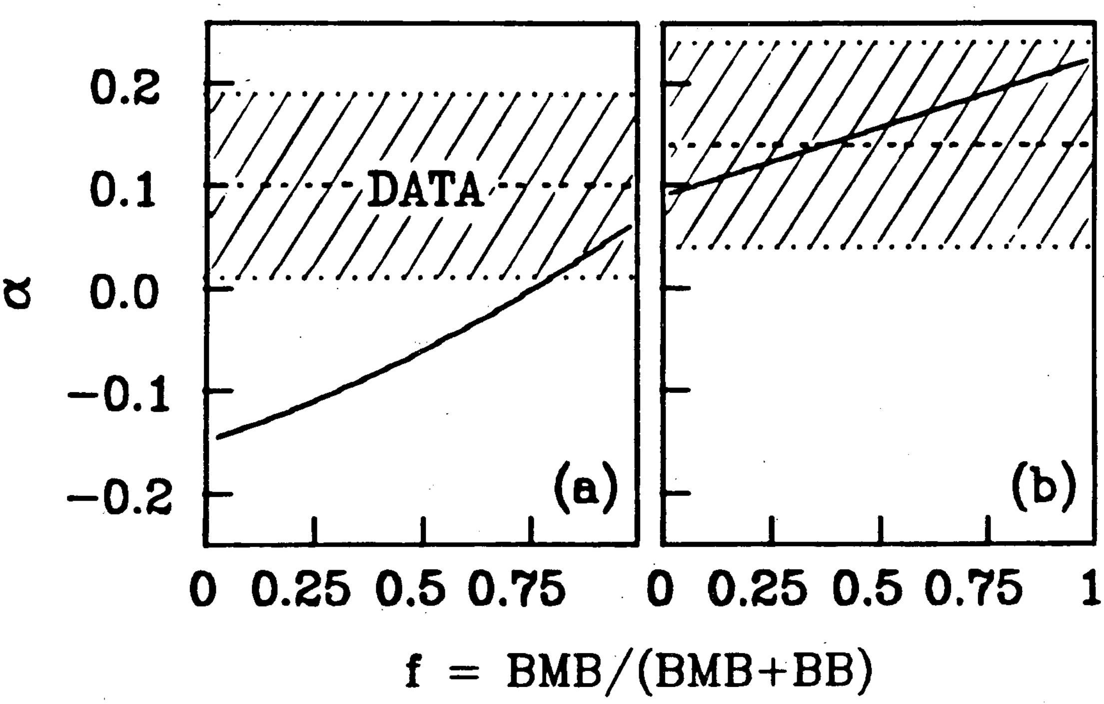

Fig. 5

XBL 854-2315

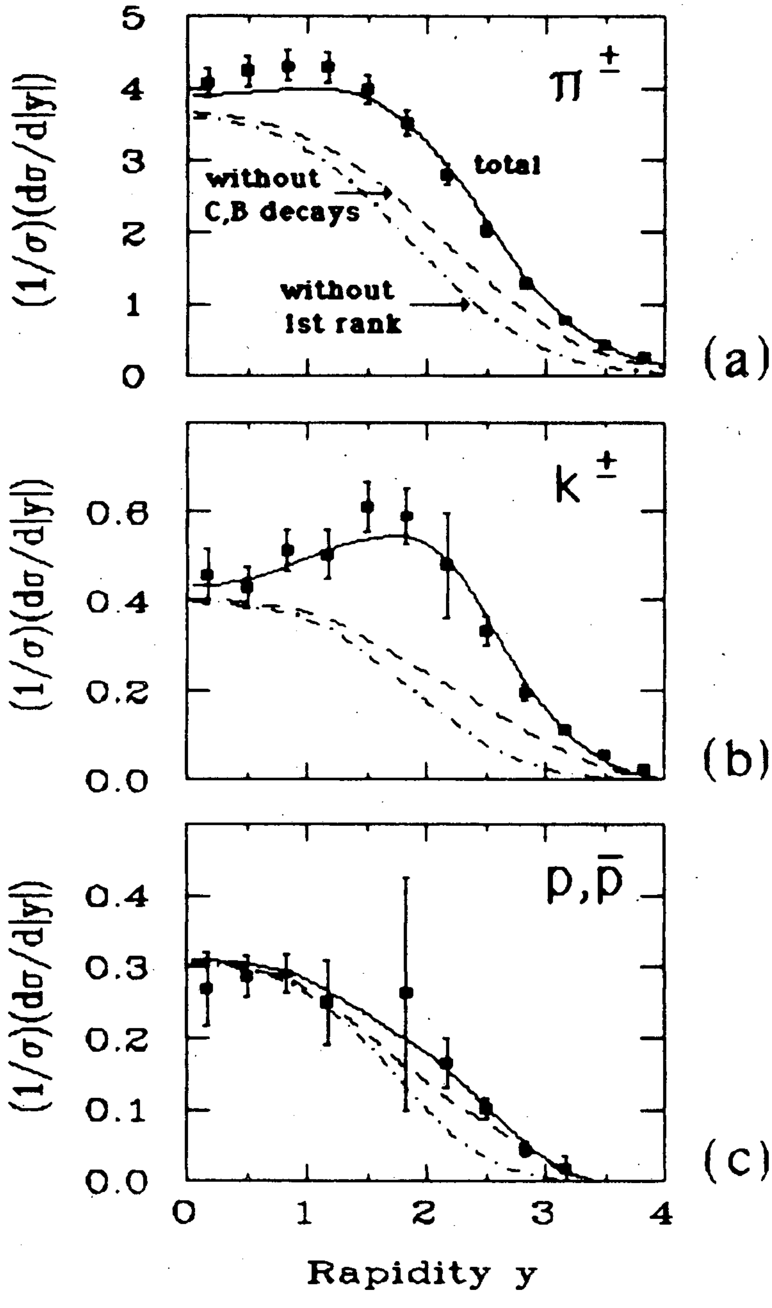

5
4
3
2
1
0
(1/σ)(dσ/d|y|)
π ±
total
without
C,B decays
without
1st rank
(a)
0.6
0.4
0.2
0.0
(1/σ)(dσ/d|y|)
K ±
(b)
0.4
0.3
0.2
0.1
0.0
(1/σ)(dσ/d|y|)
p, p̄
(c)
0
1
2
3
4
Rapidity y

Fig. 6

LAWRENCE BERKELEY LABORATORY
TECHNICAL INFORMATION DEPARTMENT
UNIVERSITY OF CALIFORNIA
BERKELEY, CALIFORNIA 94720